Disorder-immune photonics based on Mie-resonant dielectric metamaterials

Changxu Liu[1], Mikhail V. Rybin[2,3], Peng Mao[1,4], Shuang Zhang[1], and Yuri Kivshar[2,5]
[1]*School of Physics and Astronomy, University of Birmingham, Birmingham B15 2TT, UK*
[2]*ITMO University, St Petersburg 197101, Russia*
[3]*Ioffe Institute, St Petersburg 194021, Russia*
[4]*College of Electronic and Optical Engineering and College of Microelectronics, Nanjing University of Posts and Telecommunications, Nanjing 210023, China and*
[5]*Nonlinear Physics Centre, Australian National University, Canberra, ACT 2601, Australia*

Modern nanotechnology provides tools for realizing unique photonic structures with the feature size comparable or even smaller than the wavelength of light. However, the fabrication imperfections at the nanoscale inevitably introduce disorder that affects or even destroys many functionalities of subwavelength photonic devices. Here we suggest a novel concept to achieve a robust bandgap which can endure disorder beyond 30% as a result of the transition from photonic crystals to Mie-resonant metamaterials. We demonstrate photonic waveguides and cavities with strong robustness to position disorder. Utilizing Mie-resonant metamaterials with high refractive index provides an alternative approach to the bandgap-based nanophotonic devices instead of harnessing the fabrication precision, and also brings new functionalities.

The idea of manipulating the electromagnetic waves with subwavelength structures originates from the 19-th century, when Heinrich Hertz managed to control meter-long radio waves through wire-grid polarizer with centimeter spacings [1]. As the rapid advancement of the nanotechnology with fabrication resolution down to micrometer or even nanometers, a plethora of subwavelength systems with structure-induced optical properties are achieved, ranging from photonic crystals to metamaterials [2]. Among them, a photonic crystal (PhC) is a periodic optical structure that has attracted considerable interest for its ability to confine, manipulate, and guide light [3]. Spatial periodicity of the dielectric function is essential to obtain *a photonic bandgap* where the propagation for photons within a certain frequency gap is forbidden, providing unique features for a variety of applications ranging from lasers [4, 5], all-optical memories [6] to sensing [7] and emission control [8].

To achieve unparalleled functionalities with the subwavelength structures, a stringent requirement for the fabrication accuracy is required. As a result, the impact of disorder on such photonic structures has extensively been studied, both numerically and experimentally [9–36]. When the disorder is small enough (up to a few percent of the lattice constant) and can be treated as a perturbation, the interaction between the order and disorder gives rise to interesting optical transport phenomena involving multiple light scattering, diffusion and localization of light [15–22]. As disorder is increased further, the photonic bandgap is destroyed, owing to the adverse effect to the Bragg reflection [23–31]. For example, only a few percent of disorder can eliminate the bandgap of inverse opal photonic crystals [23, 24], requiring a severe demand on the quality of lattice uniformity for a good performance. Therefore, achieving a photonic bandgap robust to disorder plays a crucial role in photonic structures for a variety of applications. To the best of our knowledge, the only way to achieve good robustness is to utilize nontrivial topological properties [37], which are associated with unidirectional waveguides composed of gyromagnetic materials. However, the external magnetic field is a prerequisite to break time-reversal symmetry [38], hindering its practical application.

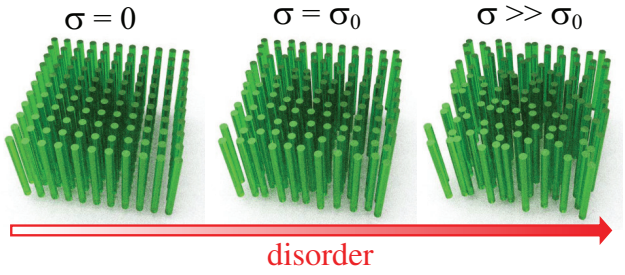

FIG. 1: Schematic of a photonic structure, composed of dielectric nanorods, with an increasing position disorder σ, respectively.

Being inspired by the recent studies of the dielectric Mie-resonant metamaterials (MMs) and their link to PhCs [39–41], here we consider photonic structures with the optically induced Mie resonances and reveal that they can support disorder-immune photonic bandgaps, in a sharp contrast with PhC where the Bragg resonances require stringent periodicity and consequently are not tolerant to disorder. Our numerical results demonstrate robustness of the optical waveguides under intense disorder, suggesting the way towards a new generation of disorder-immune photonic devices with cost-effective fabrication processes.

We start from an ideal periodic structure composed of nanorods arranged in a square lattice, as illustrated in the left panel of Fig. 1. The lattice constant is $a = 500$ nm and the rod radius is $r = 125$ nm, so that the ratio r/a defines a filling fraction of the structure. The permittivity of the nanorod is ε, with whose value identifying the system either as photonic crystals (low ε) or dielectric metamaterials (high ε) [39]. As the first step, we introduce disorder to the rod position (x^i, y^i) as: $x^i = x_0^i + \sigma U_x$ and $y^i = y_0^i + \sigma U_y$, where (x_0^i, y_0^i) is the original position in the periodic lattice, U_x and U_y are random variables distributed uniformly over the interval $[-1, 1]$, and

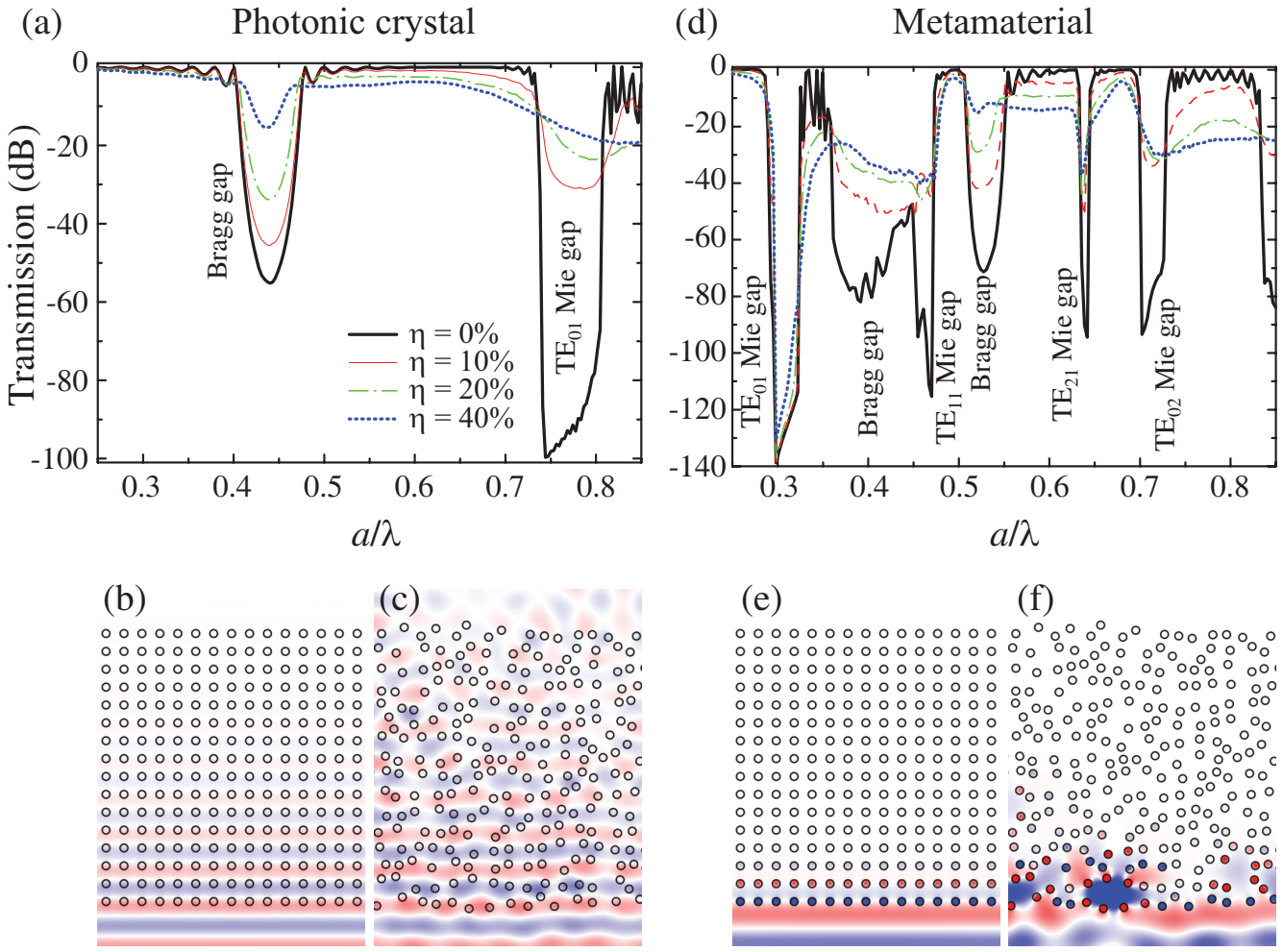

FIG. 2: Transmission spectra of (a) a photonic crystal (with $\varepsilon = 4$) and (d) a metamaterial (with $\varepsilon = 25$) with different values of the disorder parameter η. Black solid curves are perfect structures ($\eta = 0$), red dashed curves are weak disorder ($\eta = 10\%$); green dash-dot curves are moderate disorder ($\eta = 20\%$); blue dotted curves correspond to a strong disorder ($\eta = 40\%$). Origin of spectral dips are labeled. Magnetic field distribution in (c,d) photonic crystal (for $\eta = 0$ and $\eta = 40\%$, respectively) and (e,f) metamaterial (with $\eta = 0$ and $\eta = 40\%$, respectively). In each of the panels (c,d) and (e,f), the waves propagate from the bottom to the top.

the parameter σ describes the strength of the disorder. We also consider the normalized disorder strength η defined as the σ-to-a ratio expressed in %. Since the height of the nanorod is much larger than its radius, a two-dimensional approximation in the (x, y) plane is valid.

When disorder is introduced (see Fig. 1), the translational symmetry of the structure becomes broken, making the bandgap structure of the spectrum in the reciprocal space to be ill-defined. As a result, we study properties of these photonic structures in the real space assuming that the low-transmission spectral regions associated with bandgaps are still observable in the corresponding spectrum.

In the analysis of disordered media, the light propagation is characterized by a logarithmic-average transmission instead of average transmission (see Ref. [42] for details). Figure 2 demonstrates the logarithmic-averaged transmission (averaged over an ensemble of 100 samples) vs. the disorder strength η for both photonic crystals and metamaterials. In addition, we show the results for the wave propagation through the corresponding structures with a specific disorder realization for the lowest bandgap. We observe that the spectra consist of a number of pronounced dips (associated with the spectral gaps) which can be linked to either Mie and Bragg resonances. The Bragg gaps are observed as symmetric dips, while the Mie gaps have a knife-tip shape. In the regime of photonic crystals [see Fig. 2(a)], we observe a degradation of all gaps with a stronger effect manifested for the second bandgap associated with the TE_{01} Mie resonances (about 70 dB for even weak disorder $\sigma = 50$ nm or $\eta = 10\%$).

In a sharp contrast, in the regime of a metamaterial [see Fig. 2(d)], the lowest bandgap survives under even strong disorder of $\sigma = 200$ nm (or $\eta = 40\%$). In this regime, the Mie scattering from individual nanorods play a paramount role to form the bandgap through the TE_{01} Mie resonances, reducing strict requirements of periodicity. The field distributions shown in Fig. 2(e,f) reveal the effective field suppression by

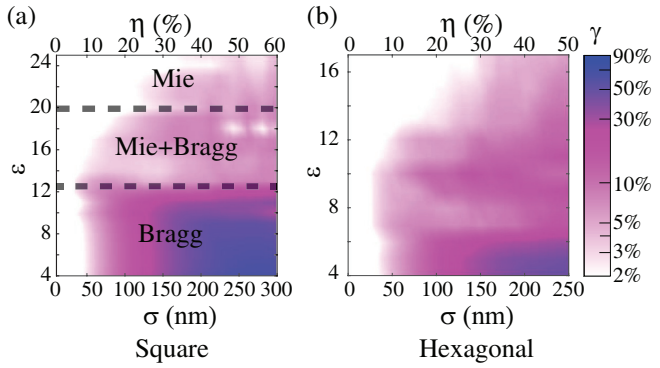

FIG. 3: Degradation of the reflection γ, as defined by Eq. (1), at different values of ε, illustrating the robustness of the structure for (a) square and (b) hexagonal lattices, respectively.

each nanorod oscillating out-of-phase with the incident wave. Remarkably, the position disorder affects all other gaps including higher-order Mie gaps. The reason is that all these gaps are above the lowest Bragg gap, so that for all such frequencies a dielectric structure of nanorods does not behave as an effective metamaterial. Thus, in spite of the identical configurations of the dielectric nanorods in Fig. 2(c) and Fig. 2(f), the wave propagation is remarkably different when the dielectric constant ϵ of each rod changes from low to higher values.

To provide a comprehensive picture of the impact of the position disorder to the system transforming from the PhC to MM regimes, we conduct a series of numerical simulations with different values of ε ranging from 4 to 25. To quantitatively represent the robustness of the photonic bandgap, we define the following parameter,

$$\gamma = (\overline{R}_0 - \overline{R})/\overline{R}_0, \tag{1}$$

where $\overline{R} = \int_{\lambda_1}^{\lambda_2} Rd\lambda/(\lambda_2 - \lambda_1)$ is the averaged reflection in the bandgap between λ_1 and λ_2. The degradation is normalized by $\overline{R}_0$, that is the reflection in the bandgap without disorder. Consequently, γ represents the deterioration of reflection in the bandgap, with a smaller value demonstrating a better robustness. Figure 3(a) summarizes the value of γ with different ε as the disorder σ increases for the bandgaps with lowest energy (as shown in Figs. 2(a) and (d). The value of γ is averaged from three different sets of the uniform random variables. The relative change to the lattice constant is also labeled by the η axis. The diagram can be unambiguously divided into three regimes. When the value of ε is small, the system operates as a PhC, corresponding to the situation shown in Figs. 2(a-c). The bandgap is quite vulnerable to the disorder, around 10% of the position disorder can break the perfection of the photonic bandgap. As the increment of the permittivity, the system transforms into a new regime, where the bandgaps is formed by the overlap of Mie and Bragg resonances [39]. The Mie scattering from individual nanorods increases the robustness to the disorder, reducing the degradation γ compared to the previous regime. Further enhancement of ε drives the lowest bandgap formed by the Mie scattering, and the system transforms into the effective MM structure with a good robustness to the position disorder. Under intense disorder, a well-defined stop band persists, as illustrated in Figs. 2(d-f). The transition of the robustness parameter γ precisely matches the phase transition from PhC to MM "phases" [39], identifying the unique role of the Mie scattering playing in the disorder-immune photonic bandgaps.

To illustrate generality of the disorder-immune photonic bandgaps, we analyze the structure robustness for a different geometry, namely a hexagonal lattice of nanorods that can support a bandgap for the TE waves [43]. In addition, a different ratio $r/a = 0.3$ is employed for the generality study while the lattice constant is kept the same, $a = 500$ nm. Figure 3(b) shows the value of γ for varying ε. A similar behavior is illustrated for a square lattice nanorods in Fig. 3(a), demonstrating three regimes with different level of robustness to the position disorder. The values of ε for achieving strong robustness is ameliorated to a smaller value around 15 due to the optimal lattice [44]. The typical transmission spectra for both PhC and MM regimes can be found in Supplementary Materials.

We further investigate the robustness effect for more practical structures such as a photonic waveguide. The waveguide is readily generated by introducing a line defect along the y-direction. For the PhC case, we select the TE_{01} Mie bandgap with a better light confinement (since the Bragg frequency has a strong angular dependence). Figures 4(a,b) illustrate the spatial distribution of the magnetic field in a disorder-impacted waveguide operating as PhC and MM, respectively, while the disorder-free example can be found in Supplementary Materials. Here the disorder parameter σ=50 nm. In spite of the disorder destroying the ideal structure, the light is still well confined in the active region [see Fig. 4(b)], demonstrating a good robustness when operating in the MM regime. With a reduced value of ε, the waveguide losses its function with the transverse diffusion under the same position configuration for a PhC, as shown in Fig. 4a. To quantitatively demonstrate the impact of disorder, we calculated the transmission T of the waveguide under different σ, as shown in Fig. 4(c). Similarly, the transmission is normalized to T_0, the value without disorder for the comparison. A definite improvement of the robustness for the waveguide is observed for the MM regime with large permittivity. In addition, a more complicated situation is investigated with a bent waveguide embedded into a hexagonal lattice, as shown in Figs. 4(d,e). Despite the vulnerability to the disorder at the corner where the propagation direction varies, the waveguide operating in the MM regime [see Fig. 4(e)] persists the function under the position disorder, compared with the PhC regime [see Fig. 4(d)]. We implement a quantitative analysis for the transmission degradation in Fig. 4(f), demonstrating the robustness enhancement from permittivity increment similar to a straight waveguide in a square lattice of nanorods shown in Fig. 4(c).

Besides waveguides, PhCs are widely used as to build optical cavities for different applications ranging from lasing to sensing. Consequently, it is crucial to clarify the robustness of an optical cavity formed by high-index dielectric rods. Here

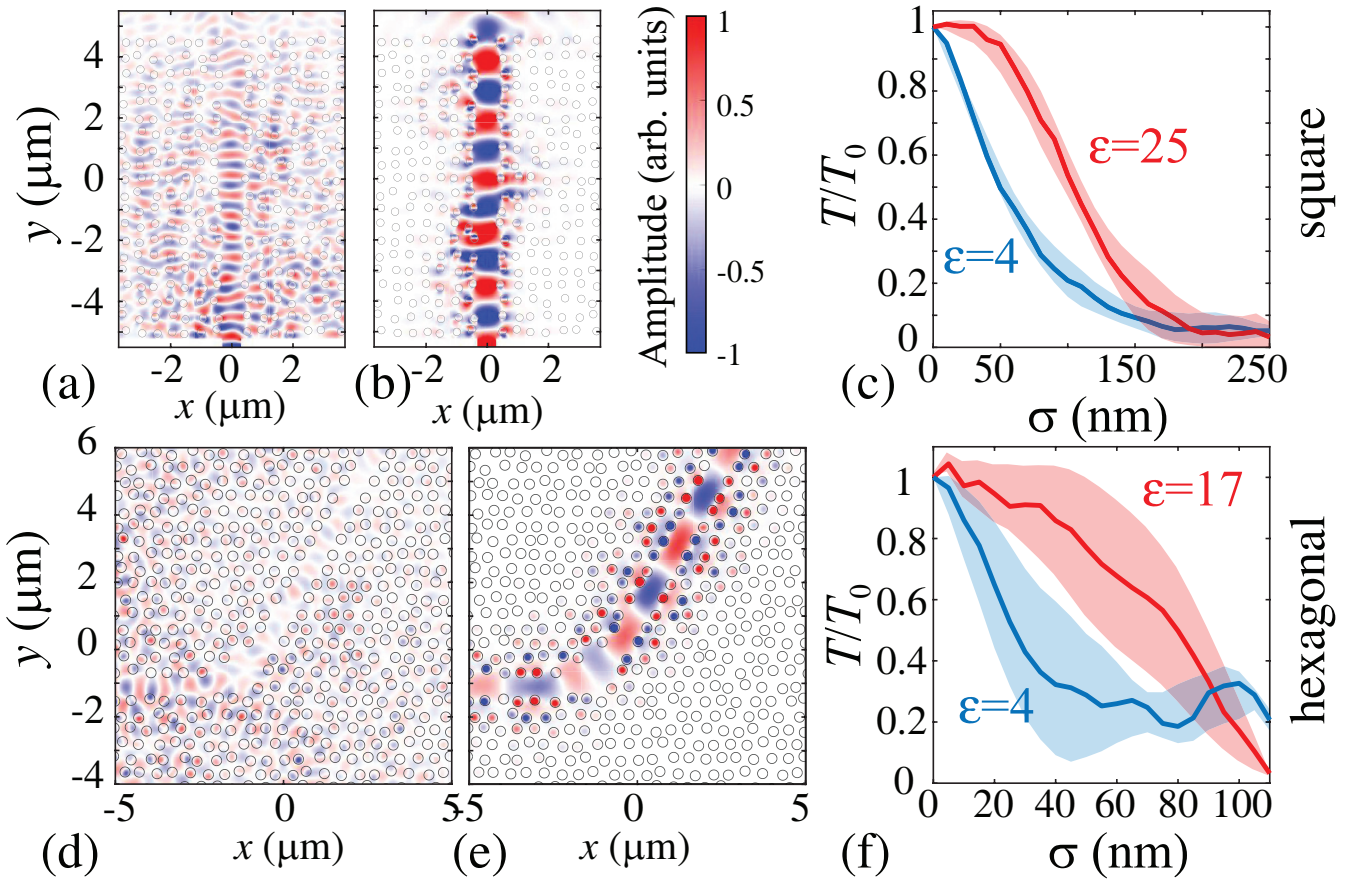

FIG. 4: (a,b) Field distribution H_z in a straight waveguide created in a square lattice of nanorods with disorder σ = 50 nm for (a) $\varepsilon = 4$ and (b) $\varepsilon = 25$. (c) The corresponding relative transmission T/T_0 vs. σ for $\varepsilon = 4$ and $\varepsilon = 25$, respectively, for a square lattice of nanorods. (d,e) Field distribution H_z in a bent waveguide created in a hexagonal lattice with disorder σ = 40 nm for (d) $\varepsilon = 4$ and (e) $\varepsilon = 17$. (f) The corresponding relative transmission T/T_0 vs. σ for $\varepsilon = 4$ and $\varepsilon = 17$, respectively, for a hexagonal lattice of nanorods.

we create an optical cavity by introducing a point defect in the hexagonal lattice, as shown in Fig. 5(a). Again, we assume that disorder is embedded in the rod position, as demonstrated in Fig. 5(a) for a perfect cavity ($\sigma = 0$, upper panel) and a disordered cavity ($\sigma = 100$ nm, lower panel).

The position fluctuations for nanorods defining the cavity boundary (circles) is intentionally eliminated to provide a fixed cavity shape. For the evaluation of the cavity robustness, we analyze the Q factor calculated as $Q = \omega_R/\Delta\omega$ through the signals from four randomly located points inside the cavity, with ω_R being the resonant frequency, and $\Delta\omega$ being FWHM parameter. Figure 5(b) demonstrates a relationship between Q and σ for both PhC and MM regimes, respectively, with the value averaged with three different sets of random variables. The Q factor is normalized to its value without disorder, Q_0, to exclude a difference between the two cases. We observe that PhC structures ($\varepsilon = 4$) are quite fragile to the disorder, whereas the photonic cavity operating in the MM regime ($\varepsilon = 15$) is more robust, only experiencing severe degradation when σ reaches 50 nm.

In addition to fluctuations in the rod positions, other types of disorder are also important for the fabrication. We study also the robustness to a size disorder and consider a photonic structure of different nanorods composed in a square lattice, as summarized in Figs. 5(c-d). Here we assume that the disorder introduces fluctuations in the rod radii, $r = r + \sigma_r U_r$, where U_r are random variables distributed uniformly over the interval $[-1, 1]$, and the disorder in the size and position are of the similar strength, so that the relative disorder is: $\eta = \sigma/a = \sigma_r/r$. Figure 5(c) shows a typical disordered structure with $\eta = 25\%$. Similarly, we use the parameter γ to evaluate the structure robustness, as shown in Fig. 5(d) for the regimes of PhC ($\varepsilon = 4$) and MM ($\varepsilon = 25$). The fluctuations in the nanorod radius cause a variation of the Mie resonance, consequently inducing deterioration of the robustness compared with the case presented in Fig. 3(a). However, even here we observe a substantial improvement of the system robustness when the system transfers from the PhC to MM regime.

In summary, we have revealed a novel regime for the scattering of light in photonic structures with robust bandgaps by transforming the structure from a photonic crystal to a meta-

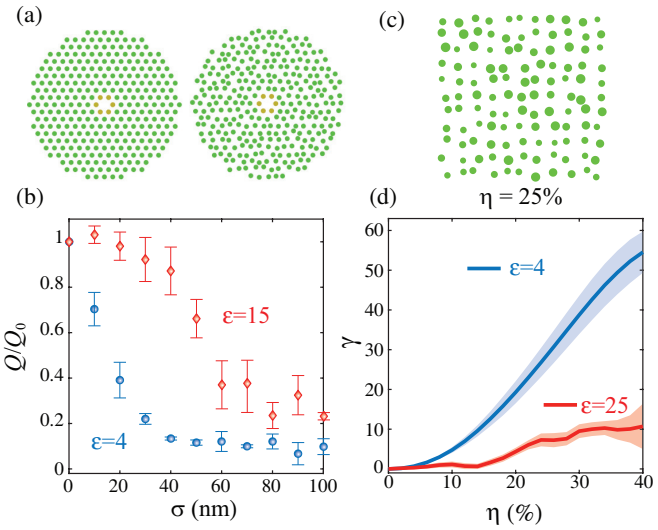

FIG. 5: (a) An optical cavity formed by a hexagonal lattice of dielectric rods without disorder (upper panel) and with disorder (lower panel). (b) Degradation of the relative quality factor Q/Q_0 with disorder σ for $\varepsilon = 4$ and $\varepsilon = 15$. (c) An example of a photonic structure with both position and size disorder, for $\eta = 25\%$. (d) Robustness parameter γ vs. disorder η for $\varepsilon = 4$ and $\varepsilon = 25$, respectively.

material. We have demonstrated that, when the Mie scattering from individual dielectric elements dominate over the Bragg scattering, both reflection and confinement of light becomes immune to an intense disorder. Such a robustness to disorder provides an alternative criterion for the transition from PhC to MM, in addition to the study of the position of the lowest bandgap [39].

Our study provides an useful guide for the nanofabrication of different photonic structures by employing dielectric metamaterials with high ε for achieving the robust bandgap regime and also lifting strict requirements on periodicity. For hexagonal lattices, one can achieve robust bandgaps from the visible to infrared spectra for GaAs [45] and Ge [46]. Importantly, such photonic structures can be realized with the bottom-up fabrication approach by utilizing the vertically aligned nanowires [47–49].

The work has partially been supported by the ERC Consolidator Grant (TOPOLOGICAL), the Royal Society, Wolfson Foundation, the Ministry of Education and Science of the Russian Federation (3.1500.2017/4.6), the Russian Foundation for Basic Research (18-02-00427), the Australian Research Council, and the European Union Horizon 2020 research innovation programme under the Marie Skłodowska-Curie Grant (No. 752102). YK thanks Th. Krauss and K. Busch for critical comments and useful discussions.

[1] F. Träger, *Springer Handbook of Lasers and Optics* (Springer Science & Business Media, 2012).
[2] P. Cheben, R. Halir, J. H. Schmid, H. A. Atwater, and D. R. Smith, *Subwavelength integrated photonics*, Nature **560**, 565 (2018).
[3] J. D. Joannopoulos, S. G. Johnson, J. N. Winn, and R. D. Meade, *Photonic Crystals: Molding the Flow of Light* (Princeton University Press, 2011).
[4] K. Hirose, Y. Liang, Y. Kurosaka, A. Watanabe, T. Sugiyama, and S. Noda, *Watt-class high-power, high-beam-quality photonic-crystal lasers*, Nature Photonics **8**, 406 (2014).
[5] S. Wu, S. Buckley, J. R. Schaibley, L. Feng, J. Yan, D. G. Mandrus, F. Hatami, W. Yao, J. Vučković, A. Majumdar, X. Xu, *Monolayer semiconductor nanocavity lasers with ultralow thresholds*, Nature **520**, 69 (2015).
[6] E. Kuramochi, K. Nozaki, A. Shinya, K. Takeda, T. Sato, S. Matsuo, H. Taniyama, H. Sumikura, and M. Notomi, *Large-scale integration of wavelength-addressable all-optical memories on a photonic crystal chip*, Nature Photon. **8**, 474 (2014).
[7] C. Fenzl, T. Hirsch, and O. S. Wolfbeis, *Photonic crystals for chemical sensing and biosensing*, Angew. Chem. Int. Ed. **53**, 3318 (2014).
[8] S. Noda, M. Fujita, and T. Asano, *Spontaneous-emission control by photonic crystals and nanocavities*, Nature Photon. **1**, 449 (2007).
[9] V. N. Astratov, A. M. Adawi, S. Fricker, M. S. Skolnick, D. M. Whittaker, and P. N. Pusey, *Interplay of order and disorder in the optical properties of opal photonic crystals*, Phys. Rev. B **66**, 165215 (2002).
[10] A. F. Koenderink and W. L. Vos, *Light exiting from real photonic band gap crystals is diffuse and strongly directional*, Phys. Rev. Lett. **91**, 213902 (2003).
[11] A. A. Zharov, I. V. Shadrivov, and Y. S. Kivshar, *Suppression of left-handed properties in disordered metamaterials*, J. Appl. Phys. **97**, 113906 (2005).
[12] S. Hughes, L. Ramunno, J. F. Young, and J. E. Sipe, *Extrinsic optical scattering loss in photonic crystal waveguides: role of fabrication disorder and photon group velocity*, Phys. Rev. Lett. **94**, 033903 (2005).
[13] J. Gollub, T. Hand, S. Sajuyigbe, S. Mendonca, S. Cummer, and D. R. Smith, *Characterizing the effects of disorder in metamaterial structures*, Appl. Phys. Lett. **91**, 162907 (2007).
[14] A. A. Asatryan, L. C. Botten, M. A. Byrne, V. D. Freilikher, S. A. Gredeskul, I. V. Shadrivov, R. C. McPhedran, and Y. S. Kivshar, *Suppression of Anderson localization in disordered metamaterials*, Phys. Rev. Lett. **99**, 193902 (2007).
[15] J. Topolancik, B. Ilic, and F. Vollmer, *Experimental observation of strong photon localization in disordered photonic crystal waveguides*, Phys. Rev. Lett. **99**, 253901 (2007).
[16] C. Toninelli, E. Vekris, G. A. Ozin, S. John, and D. S. Wiersma, *Exceptional reduction of the diffusion constant in partially disordered photonic crystals*, Phys. Rev. Lett. **101**, 123901 (2008).
[17] R. J. P. Engelen, D. Mori, T. Baba, and L. Kuipers, *Two regimes of slow-light losses revealed by adiabatic reduction of group velocity*, Phys. Rev. Lett. **101**, 103901 (2008).
[18] P. D. García, S. Smolka, S. Stobbe, and P. Lodahl, *Density of states controls Anderson localization in disordered photonic crystal waveguides*, Phys. Rev. B **82**, 165103 (2010).
[19] L. Sapienza, H. Thyrrestrup, S. Stobbe, P. D. Garcia, S. Smolka, and P. Lodahl, *Cavity quantum electrodynamics with anderson-localized modes*, Science **327**, 1352 (2010).
[20] P. D. García, R. Sapienza, C. Toninelli, C. López, and D. S. Wiersma, *Photonic crystals with controlled disorder*, Phys. Rev. A **84**, 023813 (2011).
[21] O. L. Muskens, A. F. Koenderink, and W. L. Vos, *Broadband coherent backscattering spectroscopy of the interplay between order and disorder in three-dimensional opal photonic crystals*,

Phys. Rev. B **83**, 155101 (2011).

[22] V. Savona, *Electromagnetic modes of a disordered photonic crystal*, Phys. Rev. B **83**, 085301 (2011).

[23] Z.-Y. Li and Z.-Q. Zhang, *Photonic bandgaps in disordered inverse-opal photonic crystals*, Adv. Mater. **13**, 433 (2001).

[24] Z.-Y. Li and Z.-Q. Zhang, *Fragility of photonic band gaps in inverse-opal photonic crystals*, Phys. Rev. B **62**, 1516 (2000).

[25] M. Bayindir, E. Cubukcu, I. Bulu, T. Tut, E. Ozbay, and C. M. Soukoulis, *Photonic band gaps, defect characteristics, and waveguiding in two-dimensional disordered dielectric and metallic photonic crystals*, Phys. Rev. B **64**, 195113 (2001).

[26] M. A. Kaliteevski, J. M. Martinez, D. Cassagne, and J. P. Albert, *Disorder-induced modification of the transmission of light in a two-dimensional photonic crystal*, Phys. Rev. B **66**, 113101 (2002).

[27] A. Yamilov and H. Cao, *Highest-quality modes in disordered photonic crystals*, Phys. Rev. A **69**, 031803 (2004).

[28] R. Rengarajan, D. Mittleman, C. Rich, and V. Colvin, *Effect of disorder on the optical properties of colloidal crystals*, Phys. Rev. E **71**, 016615 (2005).

[29] M. A. Kaliteevski, D. M. Beggs, S. Brand, R. A. Abram, and V. V. Nikolaev, *Stability of the photonic band gap in the presence of disorder*, Phys. Rev. B **73**, 033106 (2006).

[30] A. V. Lavrinenko, W. Wohlleben, and R. J. Leyrer, *Influence of imperfections on the photonic insulating and guiding properties of finite Si-inverted opal crystals*, Opt. Express **17**, 747 (2009).

[31] L. A. Dorado and R. A. Depine, *Modeling of disorder effects and optical extinction in three-dimensional photonic crystals*, Phys. Rev. B **79**, 045124 (2009).

[32] A. Alù and N. Engheta, *Effect of small random disorders and imperfections on the performance of arrays of plasmonic nanoparticles*, New J. Phys. **12**, 013015 (2010).

[33] D. Mogilevtsev, F. A. Pinheiro, R. R. Dos Santos, S. B. Cavalcanti, and L. E. Oliveira, *Light propagation and Anderson localization in disordered superlattices containing dispersive metamaterials: effects of correlated disorder*, Phys. Rev. B **84**, 094204 (2011).

[34] E. Maguid, M. Yannai, A. Faerman, I. Yulevich, V. Kleiner, and E. Hasman, *Disorder-induced optical transition from spin Hall to random Rashba effect*, Science **358**, 1411 (2017).

[35] M. Jang, Y. Horie, A. Shibukawa, J. Brake, Y. Liu, S. M. Kamali, A. Arbabi, H. Ruan, A. Faraon, and C. Yang, *Wavefront shaping with disorder-engineered metasurfaces*, Nature Photon. **12**, 84 (2018).

[36] A. N. Poddubny, M. V. Rybin, M. F. Limonov, and Y. S. Kivshar, *Fano interference governs wave transport in disordered systems*, Nature Commun. **3**, 914 (2012).

[37] Z. Wang, Y. Chong, J. D. Joannopoulos, and M. Soljačić, *Observation of unidirectional backscattering-immune topological electromagnetic states*, Nature **461**, 772 (2009).

[38] J. Lian, J.-X. Fu, L. Gan, and Z.-Y. Li, *Robust and disorder-immune magnetically tunable one-way waveguides in a gyromagnetic photonic crystal*, Phys. Rev. B **85**, 125108 (2012).

[39] M. V. Rybin, D. S. Filonov, K. B. Samusev, P. A. Belov, Y. S. Kivshar, and M. F. Limonov, *Phase diagram for the transition from photonic crystals to dielectric metamaterials*, Nature Commun. **6**, 10102 (2015).

[40] S. Kruk and Y. Kivshar, *Functional meta-optics and nanophotonics governed by Mie resonances*, ACS Photon. **4**, 2638 (2017).

[41] Y. Kivshar, *All-dielectric meta-optics and non-linear nanophotonics*, National Science Review **5**, 144 (2018).

[42] I. M. Lifshits, S. A. Gredeskul, and L. A. Pastur, *Introduction to the Theory of Disordered Systems* (Wiley, New York, 1988).

[43] S. G. Johnson and J. D. Joannopoulos, *Introduction to photonic crystals: Bloch's theorem, band diagrams, and gaps (but no defects)*, Photonic Crystal Tutorial pp. 1–16 (2003).

[44] S. V. Li, Y. S. Kivshar, and M. V. Rybin, *Towards silicon-based metamaterials*, ACS Photon. **5**, 4751 (2018).

[45] D. E. Aspnes, S. M. Kelso, R. A. Logan, and R. Bhat, *Optical properties of $Al_xGa_{1-x}As$*, J. Appl. Phys. **60**, 754 (1986).

[46] G. E. Jellison Jr, *Optical functions of GaAs, GaP, and Ge determined by two-channel polarization modulation ellipsometry*, Opt. Mater. **1**, 151 (1992).

[47] A. I. Persson, M. W. Larsson, S. Stenström, B. J. Ohlsson, L. Samuelson, and L. R. Wallenberg, *Solid-phase diffusion mechanism for GaAs nanowire growth*, Nature Mater. **3**, 677 (2004).

[48] S. D. Hersee, X. Sun, and X. Wang, *The controlled growth of GaN nanowires*, Nano Lett. **6**, 1808 (2006).

[49] Z. H. Wu, X. Y. Mei, D. Kim, M. Blumin, and H. E. Ruda, *Growth of Au-catalyzed ordered GaAs nanowire arrays by molecular-beam epitaxy*, Appl. Phys. Lett. **81**, 5177 (2002).